A Generalized Morphological Skeleton Transform Using both Internal and External Skeleton Points

Jianning Xu
Computer Science Department, Rowan University,
Glassboro, NJ 08028, USA

Abstract - *The morphological skeleton transform (MST) is a leading morphological shape representation scheme. In the MST, a given shape is represented as a union of all maximal disks contained in the shape. The concepts of external skeleton points and external maximal disks were introduced recently to derive so-called external shape components for shape matching purposes. In this paper, we develop a generalized morphological skeleton transform that combines the concepts of internal and external maximal disks into a unified framework. In this framework, a shape is described in terms disk components that need to be added as well as disk components that need to be removed. This framework provides a more natural way of modeling the approximation and reconstruction of binary shapes.*

Keywords: mathematical morphology, shape representation, skeleton transform, shape approximation, shape reconstruction

1 Introduction

Shape representation is an important issue in image analysis and computer vision. Efficient shape representation provides the foundation for the development of efficient algorithms for many shape-related processing tasks such as image coding, shape matching and recognition, content-based video processing, and image data retrieval.

Mathematical morphology is a shape-based approach to image processing. A number of morphological shape representation algorithms have been proposed [1-8]. The morphological skeleton transform (MST) is a leading morphological shape representation scheme [1]. In the MST, a given shape is represented as a union of all maximal disks contained in the shape. The advantages of the MST include that it has a simple and intuitive mathematical characterization as well as easy and efficient implementations. Some shape matching algorithms have been developed based on the MST [9, 10].

In a recent paper, we developed a structural shape matching algorithm that uses both internal and external shape components [11]. The internal shape components are selected from the internal maximal disks determined by a traditional MST. The external shape components are selected from the external maximal disks determined by a separate "external" skeleton transform.

In this paper, we develop a generalized morphological skeleton transform that combines the concepts of internal and external maximal disks into a unified framework. In this framework, a shape is described in terms disk components that need to be added as well as disk components that need to be removed. The positive (addition) and negative (removal) steps are applied alternately to derive the final representation of the input shape.

2 Internal and External Skeleton Transforms

We first review the standard skeleton transform. For a shape image X and a structuring element B, which is used as the unit disk, if we define size-i disk iB as $iB = B \oplus B \oplus \ldots \oplus B$ (i B's), then X can be expressed as the union of all maximal disks contained in X:

$$X = (S_N \oplus NB) \cup (S_{N\text{-}1} \oplus (N\text{-}1)B) \cup \ldots \cup (S_2 \oplus 2B) \cup (S_1 \oplus B) \cup S_0 \quad (1)$$

where

$$S_i = (X \ominus iB) \setminus ((X \ominus iB) \circ B) \quad (2)$$

and N is the largest integer such that $X \ominus NB \neq \varnothing$. Each S_i is called a skeleton subset of order i. Each skeleton point in S_i represents a maximal disk of size i contained in X. A smoothed (or approximate) version of X can be reconstructed if some lower order skeleton subsets are omitted:

$$X \circ kB = (S_N \oplus NB) \cup (S_{N\text{-}1} \oplus (N\text{-}1)B) \cup \ldots \cup (S_{k+1} \oplus (k+1)B) \cup (S_k \oplus kB), \text{ for } k \leq N. \quad (3)$$

We can also write

$$X \circ kB = (X \circ nB) \cup (S_{n\text{-}1} \oplus (n\text{-}1)B) \cup \ldots \cup (S_{k+1} \oplus (k+1)B) \cup (S_k \oplus kB), \text{ for } k < n \leq N. \quad (4)$$

A more accurate approximation $X \circ kB$ for X can be obtained from a rougher approximation $X \circ nB$ by adding additional maximal disks.

We now review the concept of external skeleton points. For the unit disk B, the reflection of B is defined as

$$B^R = \{b \mid -b \in B\}. \quad (5)$$

For a shape image X and the unit disk B, since closing operation is extensive, we have

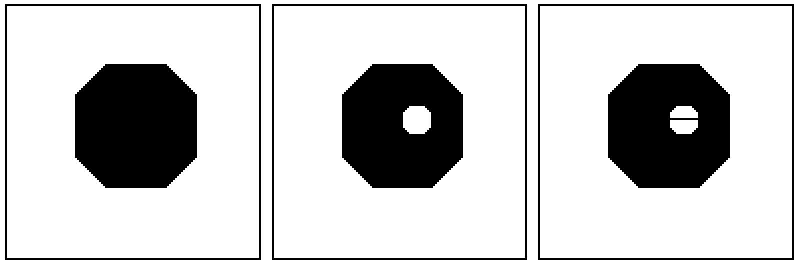

(a) (b) (c)

Fig. 1. Three simple shapes.

$$X = (X \bullet B^R) \setminus T_0 = ((X \oplus B^R) \ominus B^R) \setminus T_0$$
$$= (X_1 \ominus B^R) \setminus T_0 \qquad (6)$$

where

$$T_0 = (X \bullet B^R) \setminus X \qquad (7)$$
$$X_1 = X \oplus B^R. \qquad (8)$$

Now we can also write

$$X_1 = (X_1 \bullet B^R) \setminus T_1 \qquad (9)$$

where

$$T_1 = (X_1 \bullet B^R) \setminus X_1 = ((X \oplus B^R) \bullet B^R) \setminus (X \oplus B^R). \qquad (10)$$

Combining (6) with (9), we have

$$X = (((X_1 \bullet B^R) \setminus T_1) \ominus B^R) \setminus T_0$$
$$= ((X_1 \bullet B^R) \ominus B^R) \setminus (T_1 \oplus B) \setminus T_0$$
$$= ((((X \oplus B^R) \oplus B^R) \ominus B^R) \ominus B^R) \setminus (T_1 \oplus B) \setminus T_0$$
$$= (X \bullet 2B^R) \setminus (T_1 \oplus B) \setminus T_0. \qquad (11)$$

Each point in T_0 represents a point that is not in X and each point p in T_1 represents a disk $p \oplus B$ that is not in X. Removing all such points and disks results in the restoration of X from $X \bullet 2B^R$. Repeating similar steps, we have

$$X = (X \bullet mB^R) \setminus (T_{m-1} \oplus (m-1)B) \setminus (T_{m-2} \oplus (m-2)B) \setminus \ldots$$
$$\setminus (T_1 \oplus B) \setminus T_0 \qquad (12)$$

where

$$T_i = ((X \oplus iB^R) \bullet B^R) \setminus (X \oplus iB^R). \qquad (13)$$

The points in T_{m-1}, T_{m-2}, … T_1, T_0 can be viewed as external skeleton points and they represents external disks of different sizes. Removal of such disks results in the restoration of X from $X \bullet mB^R$. In fact, these external disks are maximal disks contained in the background shape, or the complement of X. This transform can be viewed as an external skeleton transform. A partially restored X can be created if some lower order skeleton subsets are omitted:

$$X \bullet kB^R = (X \bullet mB^R) \setminus (T_{m-1} \oplus (m-1)B) \setminus \ldots$$
$$\setminus (T_{k+1} \oplus (k+1)B) \setminus (T_k \oplus kB), \text{ for } k < m. \qquad (14)$$

A better approximation $X \bullet kB^R$ for X is obtained from a rougher approximation $X \bullet mB^R$ by removing external maximal disks.

3 Generalized Skeleton Transform

It is clear that a shape cannot be completely specified using external skeleton points only. The closed version $X \bullet mB^R$ of X in (12) in general will grow bigger as m increases. We can use a number of internal skeleton points to represent $X \bullet mB^R$. Any finite shape can be completely specified using internal skeleton points only. However, sometimes it is more efficient to describe a shape using both internal and external skeleton points. Consider the shape in Fig. 1(a). This is a near circular shape (in digital sense). Therefore, there is an efficient representation for it using internal skeleton points only. Now look at the shape in Fig. 1(b). This is the same circular shape with a near circular hole in it. If we still only use internal skeleton points, then we will need a lot more skeleton points to describe the areas between internal and external boundaries. If we can use external skeleton points to describe the hole first, then we can still use the initial efficient internal skeleton representation for the overall circular shape. Now we consider the shape in Fig. 1(c). The hole on the object has been cut into two halves. To represent two separate holes, we will need to use more external skeleton points. But if we can describe the small line segment that separates the original hole using some positive skeleton points first, then the more efficient representation for the original hole can still be used as part of the overall description. In this section, we develop a generalized skeleton transform that takes this hierarchical and alternately positive and negative description approach.

For a given shape image X and an structuring element B which is used as the unit disk, we can write

$$X = (X \circ B) \cup S_0 = X' \cup S_0 \qquad (15)$$

where

$$X' = X \circ B, \qquad (16)$$
$$S_0 = X \setminus (X \circ B). \qquad (17)$$

In (15), X' can be viewed as a smoothed version of X and S_0 is a positive skeleton subset. For X' we can write

$$X' = (X' \bullet B^R) \setminus T_0 = X_1 \setminus T_0 \qquad (18)$$

where

$$X_1 = X' \bullet B^R \qquad (19)$$
$$T_0 = (X' \bullet B^R) \setminus X' \qquad (20)$$

In (18), X_1 can be viewed as a smoothed version of X' and T_0 is a negative skeleton subset. Combining (15) and (18), we get

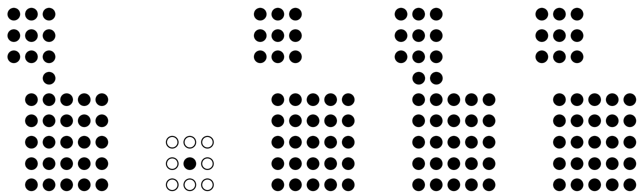

(a) (b) (c) (d) (e)

Fig. 2. An example showing that $X_1 \neq X_1 \circ 2B \cup S_1 \oplus B$: (a) Image X; (b) Unit disk B; (c) $X' = X \circ B$; (d) $X_1 = X' \bullet B^R$; (e) $X_1 \circ 2B \cup S_1 \oplus B$.

$$X = X_1 \setminus T_0 \cup S_0 \tag{21}$$

We assume that we perform set-theoretical operations from left to right. X_1 can also be viewed as a smoothed version of X and both positive and negative skeleton subsets are used to represent X now. For X_1 in (21), we have

$$X_1 \approx X_1 \circ 2B \cup S_1 \oplus B = X_1' \cup S_1 \oplus B \tag{22}$$

where

$$X_1' = X_1 \circ 2B \tag{23}$$

$$S_1 = X_1 \ominus B \setminus X_1 \ominus B \circ B \tag{24}$$

We assume that we perform morphological operations from left to right and we perform morphological operations before set-theoretical operations. In (22), X_1' is a smoothed version of X_1 and S_1 is a positive skeleton subset. Note that, in general, $X_1 \neq X_1 \circ 2B \cup S_1 \oplus B = X_1 \circ B$. An example showing this inequality is given in Fig. 2. Combining (21) and (22), we get an approximation for X:

$$X \approx X_1' \cup S_1 \oplus B \setminus T_0 \cup S_0 \tag{25}$$

Now we have an approximation for X using a smoothed version X_1' and a number of skeleton subsets. In the next step, we use closing again. For X_1' in (25), we have

$$X_1' \approx X_1' \bullet 2B^R \setminus T_1 \oplus B = X_2 \setminus T_1 \oplus B \tag{26}$$

where

$$X_2 = X_1' \bullet 2B^R \tag{27}$$

$$T_1 = X_1' \oplus B^R \bullet B^R \setminus X_1' \oplus B^R \tag{28}$$

Notice also that in general we have $X_1' \neq X_1' \bullet 2B^R \setminus T_1 \oplus B = X_1' \bullet B^R$. In (26), we have a smoothed version X_2 and a negative skeleton subset T_1. Combining (25) and (26), we have a new approximation:

$$X \approx X_2 \setminus T_1 \oplus B \cup S_1 \oplus B \setminus T_0 \cup S_0 \tag{29}$$

In order to see a pattern, we develop two more steps. The next approximation step uses an opening operation and a positive skeleton subset:

$$X_2 \approx X_2 \circ 3B \cup S_2 \oplus 2B = X_2' \cup S_2 \oplus 2B \tag{30}$$

where

$$X_2' = X_2 \circ 3B \tag{31}$$

$$S_2 = X_2 \ominus 2B \setminus X_2 \ominus 2B \circ B \tag{32}$$

A new approximation containing the new skeleton subset is

$$X \approx X_2' \cup S_2 \oplus 2B \setminus T_1 \oplus B \cup S_1 \oplus B \setminus T_0 \cup S_0 \tag{33}$$

The next approximation step uses a closing operation and a negative skeleton subset:

$$X_2' \approx X_2' \bullet 3B^R \setminus T_2 \oplus 2B = X_3 \setminus T_2 \oplus 2B \tag{34}$$

where

$$X_3 = X_2' \bullet 3B^R \tag{35}$$

$$T_2 = X_2' \oplus 2B^R \bullet B^R \setminus X_2' \oplus 2B^R \tag{36}$$

A new approximation containing the new skeleton subset is

$$X \approx X_3 \setminus T_2 \oplus 2B \cup S_2 \oplus 2B \setminus T_1 \oplus B \cup S_1 \oplus B \setminus T_0 \cup S_0 \tag{37}$$

In general, with

$$X \approx X_i \setminus T_{i-1} \oplus (i\text{-}1)B \cup S_{i-1} \oplus (i\text{-}1)B \setminus \ldots \setminus T_0 \cup S_0 \tag{38}$$

we use

$$X_i \approx X_i \circ (i+1)B \cup S_i \oplus iB = X_i' \cup S_i \oplus iB \tag{39}$$

where

$$X_i' = X_i \circ (i+1)B \tag{40}$$

$$S_i = X_i \ominus iB \setminus X_i \ominus iB \circ B \tag{41}$$

A new approximation for X containing S_i is

$$X \approx X_i' \cup S_i \oplus iB \setminus T_{i-1} \oplus (i\text{-}1)B \cup S_{i-1} \oplus (i\text{-}1)B \setminus \ldots \setminus T_0 \cup S_0 \tag{42}$$

We also use

$$X_i' \approx X_i' \bullet (i+1)B^R \setminus T_i \oplus iB = X_{i+1} \setminus T_i \oplus iB \tag{43}$$

where

$$X_{i+1} = X_i' \bullet (i+1)B^R \tag{44}$$

$$T_i = X_i' \oplus iB^R \bullet B^R \setminus X_i' \oplus iB^R \tag{45}$$

A new approximation including the latest skeleton subset is

$$X \approx X_{i+1} \setminus T_i \oplus iB \cup S_i \oplus iB \setminus T_{i-1} \oplus (i\text{-}1)B \cup S_{i-1} \oplus (i\text{-}1)B \setminus \ldots \setminus T_0 \cup S_0 \tag{46}$$

Eventually, we will encounter a N such that $X_N' = X_N \circ (N+1)B = Ø$ with $X_N \neq Ø$. This implies that $X_N \ominus (N+1)B = Ø$. And from this, we can see that $S_N = X_N \ominus NB$. It is also easy to see that $T_N = Ø$ and $X_n = X_n' = Ø$ for $n \geq N+1$. So the final approximation is

$$X \approx S_N \oplus NB \setminus T_{N\text{-}1} \oplus (N\text{-}1)B \cup S_{N\text{-}1} \oplus (N\text{-}1)B \setminus \ldots \setminus T_0 \cup S_0 \tag{47}$$

We have obtained a series of approximations for X. The final approximation uses a sequence of alternately positive and negative skeleton subsets. These skeleton subsets are obtained from progressively smoothed versions of X. We now claim that all these approximations are in fact exact representations of X:

$$\begin{aligned} X &= X' \cup S_0 \\ &= X_1 \setminus T_0 \cup S_0 \\ &= X_1' \cup S_1 \oplus B \setminus T_0 \cup S_0 \\ &= X_2 \setminus T_1 \oplus B \cup S_1 \oplus B \setminus T_0 \cup S_0 \\ &= X_2' \cup S_2 \oplus 2B \setminus T_1 \oplus B \cup S_1 \oplus B \setminus T_0 \cup S_0 \\ &= X_3 \setminus T_2 \oplus 2B \cup S_2 \oplus 2B \setminus T_1 \oplus B \cup S_1 \oplus B \setminus T_0 \cup S_0 \\ &\ldots \\ &= S_N \oplus NB \setminus T_{N\text{-}1} \oplus (N\text{-}1)B \cup S_{N\text{-}1} \oplus (N\text{-}1)B \setminus \ldots \\ &\quad \setminus T_0 \cup S_0 \end{aligned} \tag{48}$$

where X_i', X_i, S_i, and T_i are defined in (16, 17), (19, 20), (40, 41), and (44, 45).

We first show that all the approximations contain X as a subimage. Following the derivation process, we first have $X = X \circ B \cup S_0 = X' \cup S_0$ with $X' = X \circ B$. We then have $X' = X' \bullet B^R \setminus T_0 = X_1 \setminus T_0$ and $X = X_1 \setminus T_0 \cup S_0$ with $X_1 = X' \bullet B^R$. Now consider the approximation step $X_1 \approx X_1 \circ 2B \cup S_1 \oplus B$

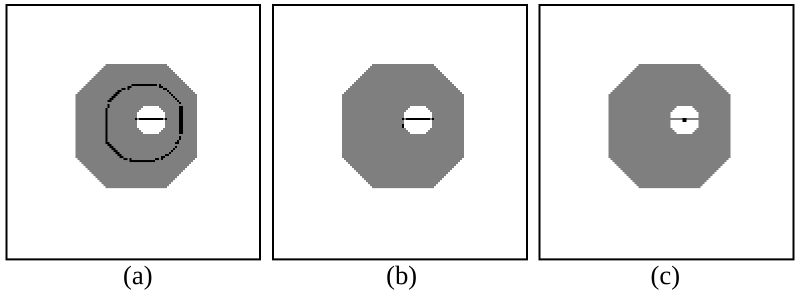

Fig. 3. The skeleton points of the standard and the new skeleton transforms.

$= X_1' \cup S_1 \oplus B$. Note that $X_1 = X' \bullet B^R \supseteq X'$ and $X_1 \circ 2B \cup S_1 \oplus B = X_1' \cup S_1 \oplus B = X_1 \circ B$ contains all size-one disks in X_1. So $X_1' \cup S_1 \oplus B$ also contains all size-one disks in X'. From $X' = X' \bullet B^R \setminus T_0$, we can see that T_0 does not contain any points in X'. Thus $X_1' \cup S_1 \oplus B \setminus T_0$ still contains all size-one disks in X'. Note also that $X' = X \circ B$ is a union of size-one disks. Therefore, $X_1' \cup S_1 \oplus B \setminus T_0 \supseteq X'$. Combining this with $X = X' \cup S_0$, we get

$$X_1' \cup S_1 \oplus B \setminus T_0 \cup S_0 \supseteq X \tag{49}$$

Consider the next approximation step $X_1' \approx X_1' \bullet 2B^R \setminus T_1 \oplus B = X_2 \setminus T_1 \oplus B$. Note that $X_1' \bullet 2B^R \setminus T_1 \oplus B = X_2 \setminus T_1 \oplus B = X_1' \bullet B^R$. Therefore

$$X_2 \setminus T_1 \oplus B \supseteq X_1' \tag{50}$$

Combining this with (49), we get $X_2 \setminus T_1 \oplus B \cup S_1 \oplus B \setminus T_0 \cup S_0 \supseteq X$. Move on to the next approximation step $X_2 \approx X_2 \circ 3B \cup S_2 \oplus 2B = X_2' \cup S_2 \oplus 2B$. Note that $X_2 = X_1' \bullet 2B^R \supseteq X_1'$ and $X_2 \circ 3B \cup S_2 \oplus 2B = X_2' \cup S_2 \oplus 2B = X_2 \circ 2B$ contains all size-two disks in X_2. So $X_2' \cup S_2 \oplus 2B$ also contains all size-two disks in X_1'. From $X_2 \setminus T_1 \oplus B \supseteq X_1'$ in (50), $T_1 \oplus B$ does not contain any points in X_1'. Thus $X_2' \cup S_2 \oplus 2B \setminus T_1 \oplus B$ still contains all size-two disks in X_1'. Note also that $X_1' = X_1 \circ 2B$ is a union of size-two disks. Therefore $X_2' \cup S_2 \oplus 2B \setminus T_1 \oplus B \supseteq X_1'$. Combining this with (49), we get $X_2' \cup S_2 \oplus 2B \setminus T_1 \oplus B \cup S_1 \oplus B \setminus T_0 \cup S_0 \supseteq X$. Repeating similar steps, we can show that all our approximations contain X as a subimage.

We now show that all our approximations are subimages of X. Consider the first representation step described in (15)-(17). Complementing the both sides of $X = X' \cup S_0$ from (15), we get $X^C = (X')^C \setminus S_0$. Complementing the both sides of (16), we have $(X')^C = X^C \bullet B^R$. We can also write S_0 in (17) as $S_0 = X \setminus X \circ B = X \cap (X \circ B)^C = X^C \bullet B^R \setminus X^C$. So, this is a representation step for X^C using a closing operation and a negative skeleton subset S_0. Now look at the next representation step described in (18)-(21). Complementing the both sides of (19) gives us $(X_1)^C = (X')^C \circ B$. From (20), we have $T_0 = X' \bullet B^R \setminus X' = X' \bullet B^R \cap (X')^C = (X')^C \setminus (X' \bullet B^R)^C = (X')^C \setminus (X')^C \circ B$. Complementing the both sides of (21), we get $X^C = (X_1)^C \cup T_0 \setminus S_0$. Clearly, this is a representation step for X^C using an opening operation and a positive skeleton subset T_0. For the next approximation step described in (22)-(25), we again first complement the both sides of (23). It gives us $(X_1')^C = (X_1)^C \bullet 2B^R$. From (24), we have $S_1 = X_1 \ominus B \setminus X_1 \ominus B \circ B = X_1 \ominus B \cap (X_1 \ominus B \circ B)^C = (X_1 \ominus B \circ B)^C \setminus (X_1 \ominus B)^C = (X_1)^C \oplus B^R \bullet B^R \setminus (X_1)^C \oplus B^R$. Complementing the both sides of (25) gives us $X^C \approx (X_1')^C \setminus S_1 \oplus B \cup T_0 \setminus S_0$. This is an approximation step for X^C using a closing operation and a negative skeleton subset S_1. Similarly, from (26)-(29), we get $(X_2)^C = (X_1')^C \circ 2B$, $T_1 = (X_1')^C \ominus B \setminus (X_1')^C \ominus B \circ B$, and $X^C \approx (X_2)^C \cup T_1 \oplus B \setminus S_1 \oplus B \cup T_0 \setminus S_0$. This is an approximation step for X^C using an opening operation and a positive skeleton subset T_1. This process can be repeated for the remaining approximation steps. Each representation/approximation step for X using an opening operation is a representation/approximation step for X^C using a closing operation and vice versa. Even though the representation/approximation sequence for X^C begins with a step using a closing operation, we can still use the similar techniques that we used earlier to show that all the approximations for X^C actually contain X^C as a subimage. That means that all the original approximations for X are subimages of X. Combined with the earlier results that all the original approximations contain X as a subimage, we conclude that all these approximations are exact representations of X.

4 Representation Examples

We now go back to the shape in Fig. 1(c). The standard skeleton transform uses 151 internal skeleton points, as shown in Fig. 3(a), to represent this shape. Our new algorithm only uses 20 internal and external skeleton points. Fig. 3(b) shows the internal skeleton points and Fig. 3(c) shows the external skeleton points of the new algorithm. In our implementation of both algorithms, we use two structuring elements B_0 and B_1 shown in Fig. 4 to define discrete disks of different sizes:

$$B = B_0 \tag{51}$$

$$iB = (i\text{-}1)B \oplus B_{(i\text{-}1) \bmod 2}, \text{ for } i \geq 2 \tag{52}$$

The skeleton subset formulas now become

(a) (b)

Fig. 4. Two structuring elements: (a) B_0; (b) B_1.

$$S_{\mathrm{i}} = X_i \ominus iB \setminus X_i \ominus iB \circ B_{i \bmod 2} \tag{53}$$

$$T_i = X_i' \oplus iB^R \bullet B^R_{i \bmod 2} \setminus X_i' \oplus iB^R \tag{54}$$

For the dog shape in Fig. 5(a), the highest order non-empty internal skeleton subset is S_{15}. $S_{15} \oplus 15B$, which is shown in Fig. 5(b), is the initial approximation to X. To improve this approximation, additional internal and external skeleton subsets are applied to add and remove points. The partial reconstruction in Fig. 5(c) is created by applying all the skeleton subsets down to order 10. Fig. 5(d) shows the reconstruction using all the skeleton subsets down to order 5. The reconstruction using all the skeleton subsets down to order 2 is shown in Fig. 5(e). The exact reconstruction is obtained if we use all the skeleton subsets. We can see that by adding and removing smaller and smaller scale parts, more and more accurate details are being created by this process. This process is similar to the creation of a clay sculpture by a sculptor. The final sculpture is created by iteratively adding and removing clay, in gradually smaller pieces, to and from the initial rough shape. The total number of internal and external skeleton points used by the generalized skeleton transform to represent the dog shape is 407. The standard skeleton transform uses 257 internal skeleton points. For many shapes, using two types of skeleton points simultaneously will cause more skeleton points to be used. However, the main advantage of the generalized skeleton transform is that it provides a more general and more powerful framework. It also provides a more natural way of modeling the approximation and reconstruction of binary shapes.

Fig. 6 shows a fractal shape and its approximations. This shape has many internal holes of various sizes. Its external boundaries also contain many structures of different scales. Fig. 6 shows the gradual reconstruction of the original shape using more and more lower-order internal and external skeleton subsets. The smallest order skeleton subsets used in these approximations are of orders 34, 20, 15, 10, 5, 2, and 1. For this shape, the standard skeleton transform uses 2363 internal skeleton points. Our new algorithm uses 1930 internal and external skeleton points. The reconstruction process agrees well with our intuitive concept of describing a shape in a gradual process of describing main structures to fine details.

5 Conclusions

We have developed a generalized skeleton transform that represents a binary shape using both internal and external skeleton points. Using this representation, a shape can be approximated at different levels. The roughest approximation is obtained by applying opening and closing operations alternately to the original shape using disk structuring elements of increasing sizes. More accurate approximations can be reconstructed by alternately adding and removing disk parts of decreasing sizes from the initial approximation. The standard skeleton transform can be seen as a special case of our algorithm. In the standard skeleton transform, only opening operations are used in deriving skeleton subsets and only “addition” (set union) operations are used to rebuild more accurate approximations.

6 References

[1] P.A. Maragos and R.W. Schafer, "Morphological skeleton representation and coding of binary images," *IEEE Trans. Acoust. Speech Signal Process.*, vol. 34, no. 5, pp. 1228-1244, 1986.

[2] I. Pitas and A.N. Venetsanopoulos, "Morphological shape decomposition," *IEEE Transactions on Pattern Analysis and Machine Intelligence.*, vol. 12, no. 1, pp. 38-45, 1990.

[3] P. Maragos, "Morphology-based symbolic image modeling, multi-scale nonlinear smoothing, and pattern spectrum," *Proc. IEEE Comput. Society Conf. Comput. Vision Pattern Recognition*, pp. 766-773, 1988.

[4] J.M. Reinhardt and W.E. Higgins, "Efficient morphological shape representation," *IEEE Transactions on Image Processing*, vol. 5, no. 1, pp. 89-101, 1996.

[5] C. Ronse and B. Macq, "Morphological shape and region description," *Signal Processing*, vol. 25, pp. 91-106, 1991.

[6] J. Goutsias and D. Schonfeld, "Morphological representation of discrete and binary images," *IEEE Transactions on Signal Processing*, vol. 39, no.6, pp. 1369-1379, 1991.

[7] J. Xu, “Efficient morphological shape representation with overlapping disk components,” *IEEE Transactions on Image Processing*, vol. 10, no. 9, pp. 1346-1356, 2001.

[8] J. Xu, Morphological decomposition of 2-D binary shapes into modestly overlapped octagonal and disk components,” *IEEE Transactions on Image Processing*, vol.16, no. 2, pp. 337-348, 2007.

[9] P. E. Trahanias, "Binary shape recognition using the morphological skeleton transform," *Pattern Recognition*, vol. 25, no. 11, pp. 1277-1288, 1992.

[10] E.A. Ei-Kwae and M.R. Kabuka, “Binary object representation and recognition using the Hilbert morphological skeleton transform,” *Pattern Recognition*, vol. 33, pp. 1621-1636, 2000.

[11] J. Xu, "Shape matching using both internal and external morphological shape components," *Proc. of 2011 International Conference on Image Processing, Computer Vision, and Pattern Recognition*,” Las Vegas, Nevada, July 2011.

[12] D. Sharvit, J. Chan, H. Tek, and B. Kimia, “Symmetry-based indexing of image databases,” *J. Visual Comm. And Image Representation*, vol. 9, no. 4, pp. 366-380, 1998.

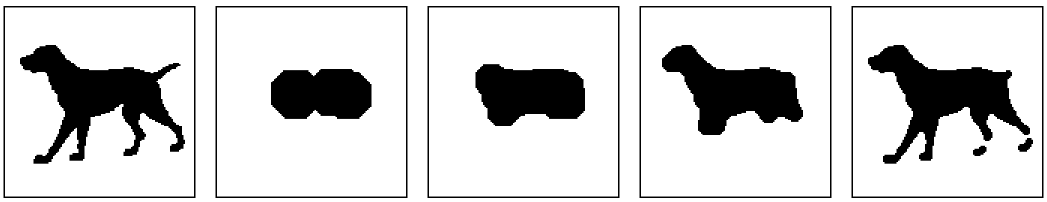

(a) (b) (c) (d) (e)

Fig. 5. A dog shape and its reconstructions.

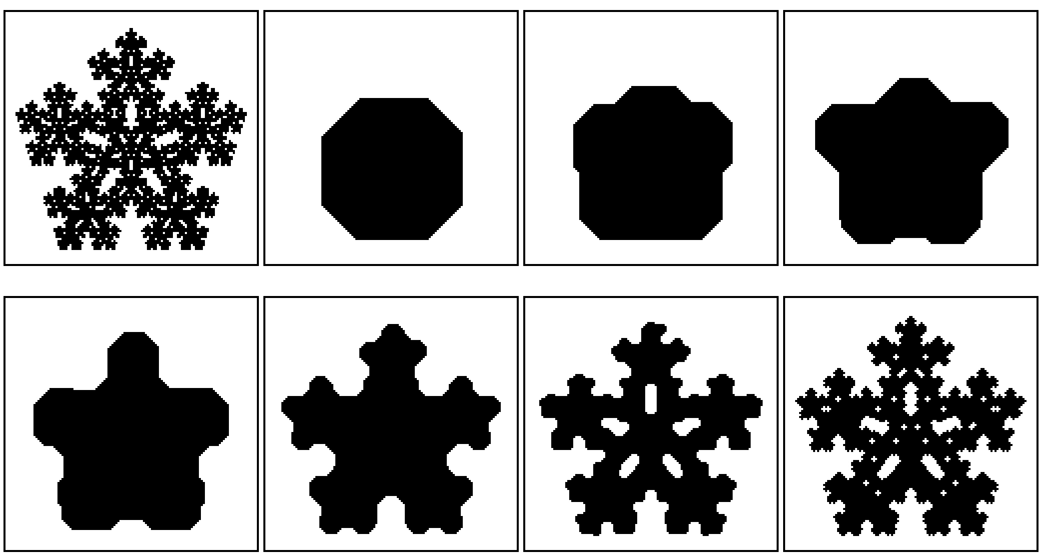

Fig. 6. A fractal shape and its reconstructions.